XeO^+ and $XeOH^+$ Ions: A New Class of Powerful Oxidative Oxygenating Agents in the Gas Phase

Antonello Filippi, Anna Troiani, and Maurizio Speranza*

Facoltà di Farmacia, Dipartimento di Studi di Chimica e Tecnologia delle Sostanze Biologicamente Attive, Università di Roma "La Sapienza", P.le A. Moro 5, 00185 Rome, Italy

Received: June 10, 1997; In Final Form: September 9, 1997[⊗]

Fourier-transform ion cyclotron resonance (FT-ICR) mass spectrometry has been used to examine ion−molecule reactions in xenon/ozone and xenon/methane/ozone mixtures. The cationic ozone derivatives, formed in these mixtures, are found to react with xenon, yielding a variety of stable products containing the Xe−O bond, i.e., XeO^+, XeO_2^+, XeO_3^+, $XeOH^+$, and $XeOH_2^+$. Estimated values for the Xe−O bond strength in the XeO^+ and $XeOH^+$ ions range around 51 and 52 kcal mol^{-1}, respectively. Both these ions exhibit distinct oxidative oxygenating properties toward some simple inorganic and organic substrates. In some representative cases, a stepwise oxidation mechanism is observed, involving the homolytic scission of a bond of the substrate by XeO^+, followed by intracomplex ion−radical recombination with elimination of the Xe fragment.

Introduction

The preparation and the characterization of polyatomic ions containing a rare gas (Rg) have attracted considerable attention since their first observation as relatively stable entities in the 1930s.[1] The importance of these species resides in the fact that they may be involved in the physics and chemistry of the low-density plasmas of interstellar clouds, planetary ionospheres, and industrial discharges. Besides, they represent the best sources for pumping chemical laser systems in the UV region of the spectrum.[2]

Despite the conceptual and practical impact of the discovery of Rg-containing polyatomic ions, very little quantitative information is available about their stability and reactivity properties. This failure is mainly caused by the inadequacy of the known procedures for generating these species in the gas phase, namely, (i) by dissociative ionization of stable Xe- and Kr-containing molecules,[3−5] (ii) by nucleophilic displacement of a leaving group (LG) from a suitable ion by Rg,[6−8] (iii) by three-body association of ions with Rg atoms at high pressures,[9−11] (iv) by ligand switching of a Rg atom from Rg_2^+ by a neutral molecule.[11−13] As a result of these approaches, it was ascertained that the stability of the Rg-containing polyatomic ions increases with charge dispersal over their structure and, therefore, with the electronegativity of the group bound to Rg.

Of course, most of the above synthetic methods are inadequate for the preparation and characterization of $RgOH_n^+$ ($n = 0, 1$) ions (Rg = Kr, Xe). The first piece of information on the occurrence of stable $XeOH_n^+$ ($n = 0, 1$) ions is due to Field and Franklin, who announced their mass spectrometric observation, together with XeO_2^+, from 70 eV electron bombardment of Xe/O_2 or H_2O mixtures.[14] By contrast, no $XeOH^+$ and XeO_2^+ ions were detected by Theard and Hamill under similar conditions, who confirmed the formation of the XeO^+ ions.[15] The krypton counterparts of the above species, i.e., KrO^+, $KrOH^+$, and KrO_2^+, have been recently prepared and characterized.[9,10,15,16]

In the present paper, we report the preparation of stable $XeOH_n^+$ ($n = 0-2$) ions by the procedure described at point ii and the evaluation of their stability and reactivity properties by Fourier-transform ion cyclotron resonance (FT-ICR) mass spectrometry. The study moved from the observation of persistent Xe-containing species arising from the reaction of the Xe atom with the $H_nO_3^+$ ($n = 1, 2$) ions,[17] easily generated in the FT-ICR source by the following reaction sequencies:

$$CH_4^+ + O_3 \rightarrow HO_3^+ + CH_3 \qquad \Delta H^\circ = -18 \text{ kcal mol}^{-1} \tag{1}$$

$$CH_5^+ + O_3 \rightarrow HO_3^+ + CH_4 \qquad \Delta H^\circ = -18 \text{ kcal mol}^{-1} \tag{2}$$

$$O_3^+ + CH_4 \rightarrow HO_3^+ + CH_3 \qquad \Delta H^\circ = -16 \text{ kcal mol}^{-1} \tag{3}$$

$$HO_3^+ + CH_4 \rightarrow H_2O_3^+ + CH_3 \qquad \Delta H^\circ = -1 \text{ kcal mol}^{-1} \tag{4}$$

Experimental Section

Materials. Ozone was produced using a Fischer 502 ozonizer, which generates a silent electric discharge in a flow of dry oxygen.[18] The ozonized gas leaving the discharge was trapped on dry silica at 195 K in order to increase the mole fraction of ozone. The O_3/O_2 mixture was allowed to reach the room temperature in a 0.5 L bulb, suitably protected against explosions, and then directly connected to the inlet line of the external source of the FT-ICR instrument. Introduction of the ozone mixture into the instrument proved difficult in that ozone is an extremely reactive molecule, which rapidly decomposes when in contact with many metallic and nonmetallic surfaces.[18] Hence, any sample of ozone introduced into the source of the mass spectrometer may easily be degraded, and a mixture of O_3 and O_2 in the source will result. Previous experimental studies indicate that this in situ degradation may exceed 10% of the O_3 present.[19] Most of the other chemicals used in the present study were commercially available and used without further purification.

Procedure. The ab initio calculations were performed using a IBM RISC/6000 version of the GAUSSIAN 94 set of programs.[20] The 3-21G basis set was employed for all the atoms

* Corresponding author. Fax No.: +39-6-49913602; E-mail: speranza@axrma.uniroma1.it.

[⊗] Abstract published in *Advance ACS Abstracts,* November 15, 1997.

S1089-5639(97)01881-1 CCC: $14.00

to optimize the geometries of the investigated species at the B3LYP level of theory,[21] as well as to obtain the corresponding thermal corrections to standard Gibbs free energies and enthalpies. (The simple harmonic oscillator model, rigid rotor approximation, and ideal gas behavior are employed.)

The FT-ICR experiments were carried out at room temperature in a Bruker Spectrospin APEX TM 47e spectrometer equipped with an external ion source and a resonance cell ("infinity cell") situated between the poles of a superconducting magnet (4.7 T). The O_3/O_2 mixture was introduced into the external source of the FT-ICR spectrometer at room temperature and at a nominal pressure ranging around 3×10^{-5} Torr. Then, either Xe or CH_4 or both ($Xe/CH_4 = 1/1$) were introduced as well through a different inlet in order to reach a total nominal pressure of ca. 8×10^{-5} Torr. Under such conditions, 70 eV electron impact on the $Xe/O_3/O_2$ mixtures readily produce the XeO^+, XeO_2^+, and XeO_3^+ ions. These species accompany formation of the $XeOH^+$ and $XeOH_2^+$ ions when electron bombardment takes place on the $CH_4/Xe/O_3/O_2$ mixtures. Under the same conditions, both HO_3^+ and $H_2O_3^+$ are readily generated from the $CH_4/O_3/O_2$ mixtures via sequences 1−4.

In most kinetic experiments, accurate measurement of the pressure of the neutral reagents placed in the internal FT-ICR reaction cell necessitates the use of an ion gauge whose sensitivity is dependent on the nature of the chemical species. The correction of the ionization gauge reading is achieved by first determining the rate constant for the reaction between the CH_4^+ radical cation and CH_4 with the FT-ICR instrument and then by comparing the obtained result with the average value of reported rate constants for this process (1.13×10^{-9} cm^3 $molecule^{-1}$ s^{-1}).[22] Subsequently, the correction factor needed for other compounds may be estimated with the method based on an indicated linear dependence of the response of the ionization gauge with the polarizability of the neutral reagent in question.[23]

The ionic plasma, generated in the external FT-ICR source, was introduced in the FT-ICR cell containing a large excess of the appropriate reagent and, then, translationally and vibrationally quenched by collisions with Ar atoms pulsed into the cell through a magnetic valve. The desired starting ions were then isolated by broad-band ejection and by "single shots"[24] and allowed to react with the appropriate neutral substrate. If involving thermal reactants, all the reactions obey a pseudo-first-order kinetics since the number of ions is roughly a factor of 10^4 lower than of the neutral substrate in the FT-ICR cell. Indeed, in all systems investigated, an inverse linear dependence is observed between the natural logarithm of the relative abundance of the starting ionic species and the reaction time, with regression analysis correlation coefficients exceeding 0.990. Thence, the second-order rate constants (k_{obs}) are derived as the ratio between the slope of linear plots and the pressure of the substrate. The major uncertainties in the conversion of the pseudo-first-order rate constants to the second-order ones reside in establishing the pressure and the temperature of the gaseous substrate, taken as that of the inlet lines and of the main vacuum system (298 K). After the above corrections for the ion gauge readings, the experimental k_{obs} values are found to be reproducible within ca. 20%. Comparison of the k_{obs} values with the corresponding collision rate constants (k_{coll}), estimated according to the trajectory calculation method,[25] provides directly the efficiency of the reaction (eff $= k_{obs}/k_{coll}$).

The collision-induced dissociation (CID) spectra of both the $^{136}XeOH^+$ and the $^{136}XeOH_2^+$ ions were obtained in the FT-ICR cell using Ar as the collision gas at ca. 1×10^{-7} Torr. The ions were accelerated by using an excitation pulse with a fixed amplitude (2 V_{p-p}) and a variable duration (0.02−0.06 ms). With variation of the duration of the excitation pulse, dissociation products were measured for different estimated laboratory kinetic energies (18−100 eV), corresponding to center-of-mass energies ranging from 4 to 21 eV.

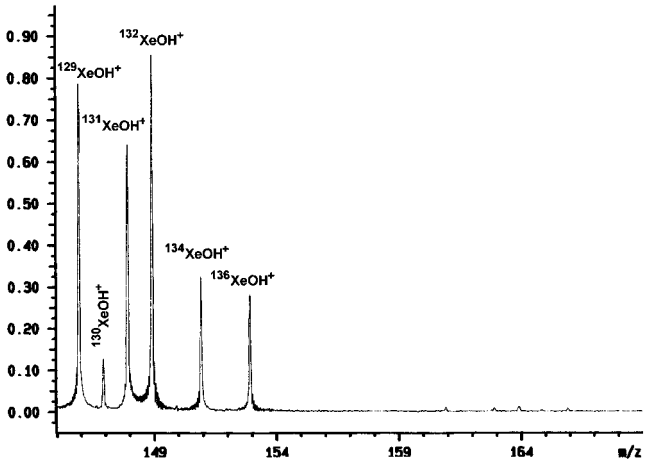

Figure 1. Detailed scanning of the region *m/z* 145−168 of the time-delayed mass spectrum ($t = 8$ s) from the isolated HO_3^+ ion reacting with xenon ($P_{Xe} = 2.6 \times 10^{-8}$ Torr) (r.i. = relative intensity with respect to the base peak).

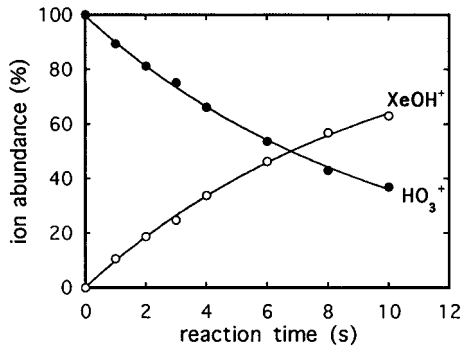

Figure 2. Time dependence of the ion abundances of the ionic products from attack of HO_3^+ on Xe ($P_{Xe} = 2.6 \times 10^{-8}$ Torr). The solid lines describe the theoretical time dependence of the relative abundance of the ionic species involved in eq 5 with $k' = 0.101$ s^{-1}).

Results

Both HO_3^+ ($H°_f = 252 \pm 3$ kcal mol^{-1}) and $H_2O_3^+$ ($H°_f = 198 \pm 5$ kcal mol^{-1}) are abundant ions produced in the $CH_4/O_3/O_2$ plasma.[17,26,27] When xenon is added to the $CH_4/O_3/O_2$ mixture, several novel ionic species containing a Xe atom are observed in significant amounts. Their actual origin was ascertained by injecting the $H_nO_3^+$ ($n = 1, 2$) ions in the FT-ICR cell containing Xe at 2.6×10^{-8} Torr.

The reaction between HO_3^+ and Xe gives rise almost exclusively to the formation of a multiplet in the *m/z* region from 146 to 153 (Figure 1). Accurate mass measurements of these signals allow unequivocal assignment of the *m/z* 146−153 multiplet to the isotopomeric $[H, O, Xe]^+$ family. The CID spectrum of the $[H, O, ^{136}Xe]^+$ ion, isolated in the FT-ICR cell from its isotopomers, displays the exclusive loss of the HO fragment, thus suggesting for $[H, O, ^{136}Xe]^+$ the $^{136}Xe-O-H$ connectivity. The dependence of the relative intensity of the HO_3^+ and $XeOH^+$ signals with the reaction time is reported in Figure 2. Best fit of the experimental ion abundances with the theoretical curves provides the first-order rate constant of reaction 5 (k' (s^{-1}) = 0.101), which can be used to calculate

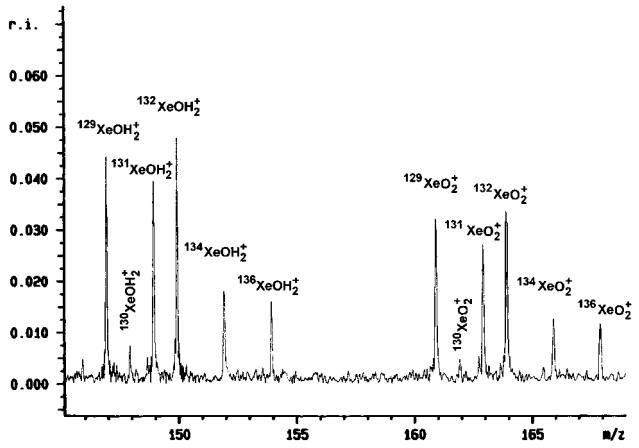

Figure 3. Detailed scanning of the region *m*/*z* 145−168 of the time-delayed mass spectrum ($t = 2$ s) from the isolated $H_2O_3^+$ ion reacting with xenon ($P_{Xe} = 2.6 \times 10^{-8}$ Torr) (r.i. = relative intensity with respect to the base peak).

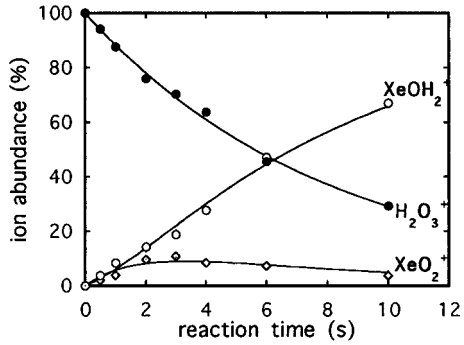

Figure 4. Time dependence of the ion abundances of the ionic products from attack of $H_2O_3^+$ on Xe ($P_{Xe} = 2.6 \times 10^{-8}$ Torr). The solid lines describe the theoretical time dependence of the relative abundance of the ionic species involved in eqs 6−8 with k' (s^{-1}) = 0.043 (eq 6), 0.080 (eq 7), and 0.017 (eq 8).

the corresponding second-order value (k_{obs} ($\times 10^{10}$ cm^3 $molecule^{-1}$ s^{-1}) = 1.23). The reaction efficiency is reported below. The same procedure has been applied to all the systems investigated.

$$HO_3^+ + Xe \rightarrow XeOH^+ + O_2 \qquad \text{eff} = k_{obs}/k_{coll} = 0.131 \tag{5}$$

The product pattern from the reaction between $H_2O_3^+$ and Xe is characterized by the formation of a multiplet in the *m*/*z* region from 147 to 154, accompanied by a less intense multiplet in the *m*/*z* region from 161 to 168 (Figure 3). Accurate mass measurements of these signals allow unequivocal assignment of the *m*/*z* 147−154 multiplet to the isotopomeric $[H_2, O, Xe]^+$ family and of the *m*/*z* 161−168 multiplet to the isotopomeric $[O_2, Xe]^+$ one. The CID spectrum of the $[H_2, O, {}^{136}Xe]^+$ ion, isolated in the FT-ICR cell from its isotopomers, displays the exclusive loss of the H_2O fragment, thus suggesting for $[H_2, O, {}^{136}Xe]^+$ the $^{136}Xe-O(H)-H$ connectivity. Analysis of the dependence of the ion abundances with the reaction time allows determination of the reaction network occurring in the FT-ICR cell (Figure 4). Accordingly, two major independent channels account for the formation $XeOH_2^+$ and XeO_2^+ ions from $H_2O_3^+$, the one involving a Xe-to-O_2 displacement (eq 6) and the other a Xe-to-OH_2 substitution (eq 7). However, close inspection of Figure 4 reveals some conversion of XeO_2^+ to $XeOH_2^+$ by reaction with ubiquitous traces of H_2O invariably present in the FT-ICR cell (eq 8).[28] Further confirmation of the specific reaction network 6−8 arises from multiple resonance experiments that allow isolation of the ion of interest (e.g., XeO_2^+) by applying appropriate frequency windows to remove all the undesired ions (e.g., $H_2O_3^+$) from the cell and by analyzing its progeny (i.e., $XeOH_2^+$) after a suitable reaction time. Coincidence of the experimental results with the theoretical curves of Figure 4 provides the first-order rate constants of the individual steps [k' (s^{-1}) (eq no.) = 0.043 (6); 0.080 (7); 0.017 (8)], which can be used to calculate the corresponding second-order values [k_{obs}($\times 10^{10}$ cm^3 $molecule^{-1}$ s^{-1}) (eq no.) = 0.53 (6); 0.97 (7); 7.05 (8)]. The relevant reaction efficiencies are reported below.

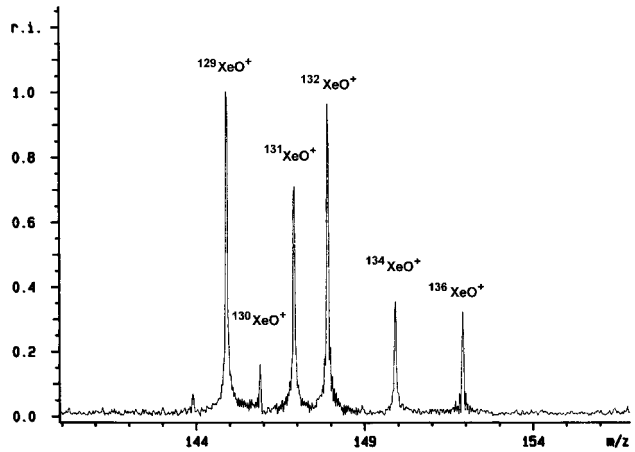

Figure 5. Detailed scanning of the region *m*/*z* 140−156 of the plasma formed in the FT-ICR external source by 70 eV electron impact on a $Xe:O_3(O_2) = 5:3$ mixture at $\sim 8 \times 10^{-5}$ Torr (r.i. = relative intensity with respect to the base peak).

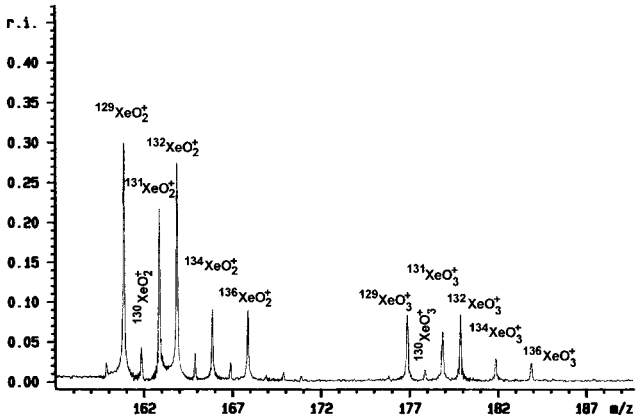

Figure 6. Detailed scanning of the region *m*/*z* 156−189 of the plasma formed in the FT-ICR external source by 70 eV electron impact on a $Xe:O_3(O_2) = 5:3$ mixture at $\sim 8 \times 10^{-5}$ Torr (r.i. = relative intensity with respect to the base peak).

$$H_2O_3^+ + Xe \rightarrow XeOH_2^+ + O_2 \qquad \text{eff} = k_{obs}/k_{coll} = 0.056 \tag{6}$$

$$H_2O_3^+ + Xe \rightarrow XeO_2^+ + H_2O \qquad \text{eff} = k_{obs}/k_{coll} = 0.103 \tag{7}$$

$$XeO_2^+ + H_2O \rightarrow XeOH_2^+ + O_2 \qquad \text{eff} = k_{obs}/k_{coll} = 0.319 \tag{8}$$

Seventy electronvolt electron impact on the $Xe/O_3/O_2$ mixtures present in the external FT-ICR source at ca. 8×10^{-5} Torr pressure yields predominantly the XeO^+ ion (Figure 5), accompanied by very minor quantities of both XeO_2^+ and XeO_3^+ (ca. 0.01% relative intensity) (Figure 6).

TABLE 1: Product Patterns and Rate Constants (k_{obs}) of the Reactions of $^{129}XeO^+$ Ions with Some Neutral Substrates

reactn no.	reaction[a]	rel yields, %	k_{obs}[b]	k_{coll}[b]	efficiency	$-\Delta H°_{rx}$[c]	footnote
(9)	$Kr \rightarrow$ no reaction						*d*
(10)	$Xe \rightarrow XeO^+ + {}^{129}Xe$	100	0.87	5.74	0.15	0	
(11a)	$D_2 \rightarrow {}^{129}XeOD^+ + D$	25	0.04	10.5	0.004	ca. 0	
(11b)	$D_2 \rightarrow {}^{129}Xe^+ + D_2O$	75	0.12		0.012	67	
(12)	$N_2 \rightarrow$ no reaction						*e*
(13a)	$CO \rightarrow {}^{129}Xe^+ + CO_2$	92	0.49	7.0	0.07	77	
(13b)	$CO \rightarrow CO_2^+ + {}^{129}Xe$	8	0.05		0.01	39	
(14)	$HCl \rightarrow HClO^+ + {}^{129}Xe$	100	0.75	12.2	0.06		*f*
(15)	$Cl_2 \rightarrow Cl_2O^+ + {}^{129}Xe$	100	1.94	7.32	0.26		*g*
(16)	$H_2O \rightarrow H_2O_2^+ + {}^{129}Xe$	100	5.79	22.3	0.26		*h*
(17a)	$NF_3 \rightarrow {}^{129}Xe^+ + NF_3O$	89	0.49	5.8	0.084	19	
(17b)	$NF_3 \rightarrow NF_2O^+ + {}^{129}XeF$	11	0.05		0.009	8	*i*
(18)	$CH_4 \rightarrow {}^{129}XeOH^+ + CH_3$	100	0.60	9.95	0.06	ca. 0	
(19)	$CHF_3 \rightarrow$ no reaction						*j*

[a] The neutral species formed in these reactions are not detected with the present experimental method, and only the elemental compositions of the expected neutral products are given. [b] $k_{obs} \times 10^{10}$ cm^3 molecule^{-1} s^{-1}; uncertainty range: ca. 20%. $k_{coll} \times 10^{10}$ cm^3 molecule^{-1} s^{-1}, calculated according to: Su, T.; Chesnavitch, W. J. *J. Chem. Phys.* **1982**, *76*, 5138. [c] $\Delta H°_{rx}$, in kcal mol^{-1}; uncertainty range ±7 kcal mol^{-1}. [d] $-\Delta H°_{rx}$ (kcal mol^{-1}) = −57 (with $KrO^+ + Xe$, as the products) (ref 16). [e] $-\Delta H°_{rx}$ (kcal mol^{-1}) = −11 (with $N_2O^+ + Xe$, as the products) (ref 27). [f] $-\Delta H°_{rx}$ (kcal mol^{-1}) = 29 ($ClOH^+$) (ref 29, 35); 53 ($HClO^+$) (ref 35). [g] $-\Delta H°_{rx}$ (kcal mol^{-1}) = 18 ($ClOCl^+$) (ref 29); 17 ($ClClO^+$) (ref 33). [h] $-\Delta H°_{rx}$ (kcal mol^{-1}) = 21 ($HOOH^+$) (ref 29, 32): −3 (H_2OO^+) (ref 33). [i] Using a MP2(FULL)/6-31G* calculated $H°_f(NF_2O^+)$ = 235 kcal mol^{-1} (ref 36); $-\Delta H°_{rx}$ (kcal mol^{-1}) = 8 (^{129}XeF); 4 ($^{129}Xe + F$) (ref 29). [j] $-\Delta H°_{rx}$ (kcal mol^{-1}) = 41 (with $CF_2O^+ + HF$, as the products) (ref 29).

TABLE 2: Product Patterns and Rate Constants (k_{obs}) of the Reactions of $^{136}XeOH^+$ Ions with Some Neutral Substrates

reactn no.	reaction[a]	rel yields, %	k_{obs}[b]	k_{coll}[b]	efficiency	$-\Delta H°_{rx}$[c]	footnote
(20)	$Xe \rightarrow$ no reaction						*d*
(21)	$CO \rightarrow CO_2H^+ + {}^{136}Xe$	100	0.02	6.95	0.002	71	*e*
(22)	$HCl \rightarrow$ no reaction						*f*
(23)	$Cl_2 \rightarrow Cl_2OH^+ + {}^{136}Xe$	100	0.24	7.26	0.03		*g*
(24)	$H_2O \rightarrow H_3O_2^+ + {}^{136}Xe$	100	0.35	22.3	0.016	9	*h*
(25)	$CO_2 \rightarrow$ no reaction						
(26)	$BF_3 \rightarrow$ no reaction						
(27)	$NF_3 \rightarrow$ no reaction						*i*
(28)	$CH_4 \rightarrow$ no reaction						*j*
(29a)	$CH_3F \rightarrow CH_3O^+ + {}^{136}Xe + HF$	65	0.02	18.0	0.002	75	*k*
(29b)	$CH_3F \rightarrow CH_2FO^+ + {}^{136}Xe + H_2$	35	0.01		0.002	51	*l*
(30)	$CHF_3 \rightarrow CHF_2O^+ + {}^{136}Xe + HF$	100	0.03	12.7	0.002	84	*m*
(31)	$CF_4 \rightarrow$ no reaction						

[a] The neutral species formed in these reactions are not detected with the present experimental method, and only the elemental compositions of the expected neutral products are given. [b] $k_{obs} \times 10^{10}$ cm^3 molecule^{-1} s^{-1}; uncertainty range ca. 20%. $k_{coll} \times 10^{10}$ cm^3 molecule^{-1} s^{-1}, calculated according to: Su, T.; Chesnavitch, W. J. *J. Chem. Phys.* **1982**, *76*, 5138. [c] $\Delta H°_{rx}$, in kcal mol^{-1}; uncertainty range ±3 kcal mol^{-1}. [d] $\Delta H°_{rx}$ (kcal mol^{-1}) = 0 (with $XeOH^+ + {}^{136}Xe$, as the products). [e] CO_2H^+═$OCOH^+$. [f] $-\Delta H°_{rx}$ (kcal mol^{-1}) = 22 (with $ClOH_2^+ + {}^{136}Xe$, as the products) (ref 37). [g] $\Delta H°_{rx}$ (kcal mol^{-1}) ≤ 0, if $H°_f(ClClOH^+) \leq 237$ kcal mol^{-1}, i.e., if $PA(ClClO) \geq 148$ kcal mol^{-1}. [h] $H_3O_2^+$═H_2OOH^+. [i] $-\Delta H°_{rx}$ (kcal mol^{-1}) = 36 (with $NF_2O^+ + HF + {}^{136}Xe$, as the products) (refs 29, 36). [j] $-\Delta H°_{rx}$ (kcal mol^{-1}) = 101 (with $CH_3OH_2^+ + {}^{136}Xe$, as the products) (ref 29). [k] $-\Delta H°_{rx}$ (kcal mol^{-1}) = 75 (CH_2OH^+), 42 (CH_3O^+) (ref 29). [l] Using the HF/4-31G calculated $H°_f(CHFOH^+)$ = 127 kcal mol^{-1} value (ref 39). [m] CHF_2O^+═CF_2OH^+ (ref 29).

The product patterns from the attack of the $^{129}XeO^+$ and the $^{136}XeOH^+$ ions on some representative substrates are reported in Tables 1 and 2, respectively.

The neutral species formed in these reactions are not detected with the present experimental method, and only the elemental compositions of the expected neutrals are given in the equations of Tables 1 and 2. The $^{129}XeO^+$ ion is found to react with all the selected neutral substrates (NS's), except Kr, N_2, and CHF_3 (Table 1). As frequently observed for other Rg molecular ions,[13] the $^{129}XeO^+$ ion mainly react with a neutral substrate (NS) by NS-to-^{129}Xe ligand switching to yield NSO^+ (e.g., eq 14 (NS = HCl)). When the recombination energy (RE) of the NSO^+ product exceeds the ionization potential (IP) of xenon, the reaction gives rise to $^{129}Xe^+$ and NSO (e.g., eq 13a (NS = CO). A similar behavior is observed for the $^{136}XeOH^+$ ion, which however appears much less reactive (Table 2). In fact, slow NS-to-^{136}Xe ligand switching is observed only with NS = CO (eq 21), Cl_2 (eq 23), or H_2O (eq 24). Loss of ^{136}Xe is sometimes accompanied by release of a small molecule (e.g., HF or H_2 in eqs 29 and 30). In this connection, it should be noted that the CHF_3 molecule is completely inert toward $^{129}XeO^+$, whereas it slowly reacts with the $^{136}XeOH^+$ ion. In all investigated reactions involving $^{136}XeOH^+$, no loss of $^{136}Xe^+$ is observed.

Discussion

Nature and Thermochemistry of the XeO^+ and $XeOH^+$ Ions. Electron impact of $Xe/O_3/O_2$ mixtures in the external FT-ICR source (ca. 8×10^{-5} Torr) generates Xe^+, O_3^+, and O_2^+ as the primary ions. The O_3^+ ion (RE = 12.43 eV) may readily lose its charge after few collisions with the present neutrals, i.e., Xe (IP(Xe) = 12.13 eV) and O_2 (IP(O_2) = 12.06 eV), yielding high-order Xe^+ and O_2^+.[13] Since O_2^+ is completely inert toward the present neutrals,[13] the abundant XeO^+ formed in the external FT-ICR source is thought to arise from extensive dissociation of the $[O_3 \cdot Xe]^+$ encounter complex formed by reactive collision between Xe^+ and O_3 or, possibly, O_3^+ and Xe. Thus, the efficient formation of XeO^+ in the FT-ICR source is taken as an indication that these processes are thermochemically allowed and, therefore, that $H°_f(XeO^+) \leq H°_f(Xe^+) + H°_f(O_3) - H°_f(O_2)$, namely, that $H°_f(XeO^+) \leq 314$ kcal mol^{-1}.[29]

The observation of stable XeO^+ and $XeOH^+$ in the diluted gas state is consistent with their B3LYP/3-21G calculated dissociation enthalpies and free energies, reported in Table 3.[30]

By combining the computed 298 K Xe−O bond energy in $XeOH^+$ ($D°(Xe^+-OH)$ = 52 kcal mol^{-1}) with the experimental heats of formation of Xe^+ ($H°_f(Xe^+)$ = 279.7 kcal mol^{-1})[29]

TABLE 3: B3LYP/3-21G Geometries, Standard Enthalpies, and Free Energies (in au)

species	$\langle s^2 \rangle$	H_{298}	G_{298}	Xe−O (Å)	O−H (Å)	Xe−O−H angle (deg)
$XeO^+(^2\Pi)$	0.7660	−7277.773 023	−7277.800 582	2.081		
$XeOH^+(^1A')$	0.0000	−7278.432 606	−7278.461 792	2.107	1.021	106.14
$Xe^+(^2P)$	0.7501	−7203.058 066	−7203.077 984			
$OH(^2\Pi)$	0.7513	−75.292 423	−75.312 735		1.018	
$O(^1D)$	0.0000	−74.552 557	−74.568 833			
$O(^3P)$	2.0005	−74.657 935	−74.675 247			
$H(^2S)$	0.7500	−0.494 951	−0.507 966			

and OH ($H°_f$(OH)=9.3 kcal mol^{-1}),[29] we estimate a *theoretical* enthalpy of formation for the $XeOH^+$ ion of ca. 237 kcal mol^{-1}, a value which is consistent with the occurrence of both the Xe-to-O_2 switching reaction 5 on HO_3^+ ($\Delta H°$ (kcal mol^{-1}) = −15 ± 3) and of the analogous H_2O-to-^{136}Xe reaction 24 on $^{136}XeOH^+$ by H_2O ($\Delta H°$ (kcal mol^{-1}) = −9 ± 3) (Table 2).

As shown in eqs 11a and 18 of Table 1, the $^{129}XeOH^+$ and $^{129}XeOD^+$ ions are obtainable also by reaction of $^{129}XeO^+$ with suitable hydron atom donors, such as CH_4 or D_2, respectively. However, while D_2 displays a very poor deuterium loss efficiency (eff = 0.004), a 15-fold increase in donor efficiency is exhibited by CH_4. This effect would suggest that the attack of thermalized $^{129}XeO^+$ on both donors is approximately thermoneutral. The data reported in Table 3 are consistent with this conclusion. In fact, the computed 298 K O−H bond energy of $XeOH^+$ ($D°(XeO^+-H)$ = 102 kcal mol^{-1}) is comparable with the experimental bond energy in D_2, 106 kcal mol^{-1},[29] and CH_4, 105 kcal mol^{-1},[29] thus pointing to the hydron atom transfer from D_2 and CH_4 to $^{129}XeO^+$ as essentially thermoneutral. On these grounds, our judgment is that the $H°_f(XeO^+)$ should range around 289 kcal mol^{-1}, in agreement with the above proposed $H°_f(XeO^+) \leqslant 314$ kcal mol^{-1} upper limit.[29] The standard reaction enthalpy values ($\Delta H°_{rx}$) listed in Tables 1 and 2 are calculated by taking $H°_f(XeOH^+)$ = 237 kcal mol^{-1} and $H°_f(XeO^+)$ = 289 kcal mol^{-1}. Accordingly, the Xe^+-O bond energy in $XeOH^+$ and XeO^+ is calculated to be as large as 52 and 51 kcal mol^{-1}, respectively. These values well compare with the experimental bond energies of XeF^+ ($D°(Xe^+-F)$ = 48 kcal mol^{-1})[5] and $XeCH_3^+$ ($D°(Xe-CH_3^+)$ = 55.2 ± 2.5 kcal mol^{-1}).[6a] In this connection, it is worth noting that the thermochemically estimated bond energy in XeO^+value is 15 kcal mol^{-1} higher than the computed 298 K value, 36 kcal mol^{-1}, inferred from the enthalpy data of Table 3. A possible reason from such a discrepancy may reside in an inadequate description of the triplet state of O at the level of theory employed.[31]

Reactivity of the XeO^+ Ions. As aforementioned, ligand exchange with loss of the ^{129}Xe atom is a major pathway followed by $^{129}XeO^+$ when colliding with some neutral substrates (NS's) under the FT-ICR conditions (Table 1). The reaction may be regarded as an oxidation via direct O^+ ion transfer from $^{129}XeO^+$ to NS. In this case, the $[N-S-O]^+$ = $[H-Cl-O]^+$, $[Cl-Cl-O]^+$, and $[H_2O-O]^+$ isomeric forms would be formed from NS = HCl (eq 14), Cl_2 (eq 15), and H_2O (eq 16), respectively (mechanism 32). Another conceivable route would involve an oxidation step preceded by homolytic bond scission in NS (mechanism 33).

$$^{129}XeO^+ + NS \rightarrow {}^{129}Xe + [N-S-O]^+ \qquad (32)$$

$$^{129}XeO^+ + NS \rightarrow [{}^{129}Xe-O-N^+\cdot S] \rightarrow {}^{129}Xe + [N-O-S]^+ \qquad (33)$$

In the latter case, formation of the $[N-O-S]^+$ = $[H-O-Cl]^+$, $[Cl-O-Cl]^+$, and $[H-O-O-H]^+$ isomeric forms is expected from the same substrates. With NS = HCl, discrimination between mechanisms 32 and 33 is prevented since both are thermochemically allowed (footnote *g* in Table 1).[29,32] However, with NS = H_2O, while path 33 is 21 kcal mol^{-1} exothermic, the alternative pathway 32 would be 3 kcal mol^{-1} endothermic (footnote *h* in Table 1).[33] Therefore, in consideration of the substantial activation energy separating $[H_2O-O]^+$ from $[H-O-O-H]^+$ (E^* = 37 kcal mol^{-1}),[33] the considerable efficiency of the oxidation of H_2O by $^{129}XeO^+$ (eq 16, eff = 0.26) suggests that the reaction very likely proceeds through mechanism 33. The same conclusion is reached in the systems with NS = HCl.[34] In fact, path 33 is calculated to be 29 kcal mol^{-1} exothermic, whereas the alternative pathway 32 is estimated ca. 53 kcal mol^{-1} endothermic (footnote *f* in Table 1).[35] With NS = D_2 (eqs 11a,b) and CH_4 (eq 18), occurrence of the stepwise sequence 33 is witnessed by the actual observation of its first step. In eqs 11a,b, the $^{129}XeOD^+$ intermediate is accompanied by the formation of $^{129}Xe^+$. This denotes that, depending upon the lifetime of the relevant adducts, the D atom is able to displace the ^{129}Xe atom from the $^{129}XeOD^+$ moiety. The same process involving the CH_3 radical seems prevented, as testified by the lack of any detectable $[C, H_4, O]^+$ fragment from eq 18.

With NS = D_2, CO, and NF_3, where $RE(NSO^+) > RE(Xe^+)$, the ligand-exchange reaction gives rise to $^{129}Xe^+$ and NSO (eqs 11b, 13a, and 17a). When NS = NF_3, the major ionic product, i.e., $^{129}Xe^+$ (eq 17a), is accompanied by minor amounts of NF_2O^+ (eq 17b). Formation of this latter product from $^{129}XeO^+$ and NF_3 is 4 kcal mol^{-1} exothermic if releasing the separated ^{129}Xe and F atoms, whereas it is 8 kcal mol^{-1} exothermic if involving the loss of the ^{129}XeF radical (footnote *i* in Table 1). The observation of the NF_2O^+ ion implies that $RE(NF_2O^+) < IP(Xe) = 12.13$ eV[29] and, therefore, $H°_f(NF_2O) > -45$ kcal mol^{-1}. In this connection, it is worth noting that reactions 17 represent a singular case of the Lewis-acid-catalyzed NF_3 oxidative oxygenation first proposed by Cacace and co-workers on the grounds of ion−molecule experiments[36] and recently proved experimentally by Christe in heterogeneous mixtures at 80 atm and $T > 150$ °C.[37] The singularity of the NF_3 oxidative oxygenation route 17b is that it involves a reactant, i.e., $^{129}XeO^+$, which plays the 2-fold role of the oxygen donor and of the Lewis-acid catalyst by transferring the O^+ moiety while accepting the F^- one (structure **I**).

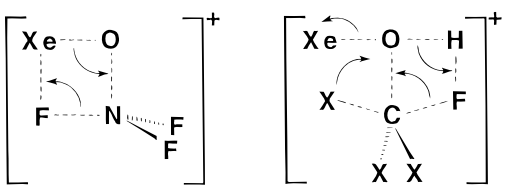

(I) (II)

Reactivity of the $XeOH^+$ Ions. Ligand exchange with loss of the ^{136}Xe atom is the only pathway observed when $^{136}XeOH^+$ collides with the selected neutrals NS under the FT-ICR conditions (Table 2). Compared to the same processes involving

$^{129}XeO^+$, the reaction appears much less efficient, as testified by the lack of any detectable Xe-to-^{136}Xe isotopic scrambling in the collision between $^{136}XeOH^+$ and natural xenon gas. Accordingly, while $^{129}XeO^+$ is found to react efficiently with D_2, HCl, NF_3, and CH_4, the $^{136}XeOH^+$ ion appears fully inert toward these substrates. Among the selected neutrals, only CO (eq 21), Cl_2 (eq 23), and H_2O (eq 24) are able to slowly displace ^{136}Xe from $^{136}XeOH^+$. Irrespective of the specific ligand exchange mechanism, whether direct (mechanism 32) or stepwise (mechanism 33), the attack of CO and H_2O on $^{136}XeOH^+$ would yield the $[O-C-O-H]^+$ and $[H-O(H)-O-H]^+$ structures, respectively. Instead, two different isomeric products would be expected from Cl_2-to-^{136}Xe on $^{136}XeOH^+$, namely, $[Cl-Cl-O-H]^+$ from direct ligand displacement (mechanism 32) and $[Cl-O(H)-Cl]^+$ from the stepwise one (mechanism 33). No direct indication about the actual structure formed in this reaction is presently available. However, to be thermochemically accessible from attack of $^{136}XeOH^+$ on Cl_2 (eq 23), the Cl_2OH^+ ion must have a standard formation enthalpy below 237 kcal mol^{-1}. This enthalpy value corresponds to a proton affinity (PA) at the O atom of Cl_2O exceeding 148 kcal mol^{-1}, in good agreement with the PA = 152 and 154 kcal mol^{-1}, calculated for the O center of ClO[29] and HOCl,[38] respectively.

Despite its comparatively low reactivity, the $^{136}XeOH^+$ ion is able to oxidize fluoromethanes. Thus, both $[C, H_3, O]^+$ and $[C, H_2, F, O]^+$ are formed from CH_3F (eq 29), while $[C, H, F_2, O]^+$ is exclusively obtained from CHF_3 (eq 30). No reaction is observed with CF_4. This behavior, coupled with the unreactivity of $^{129}XeO^+$ toward CHF_3, suggests a fluoromethane oxidative oxygenation mechanism by $^{136}XeOH^+$ promoted by the extrusion of a very stable molecule (either HF or H_2). In view of the lack of reactivity of $^{129}XeO^+$ toward CHF_3 (eq 19), a hydrogen contained in these fragments necessarily comes from $^{136}XeOH^+$. Another essential requirement for allowing fluoromethane oxidative oxygenation by $^{136}XeOH^+$ concerns the specific ligand exchange process in the $[^{136}XeOH{\cdot}CX_3F]^+$ (X = H, F) adduct (**II**). The lack of reactivity of $^{136}XeOH^+$ toward CF_4 (X = F) indicates that elimination of the ^{136}Xe ligand requires the concerted conversion of the CX_3O^+ moiety to the much more stable CX_2OX^+ by C-to-O 1,2-X migration. While this migration take place readily when X = H, it is prevented when X = F owing to the very poor migratory aptitude of fluorine in carbocations.

Conclusions

Stable $[H_n, O, Xe]^+$ (n = 0−2) can be conveniently synthesized in a FT-ICR source from ionization of $Xe/O_3/O_2$ and $CH_4/Xe/O_3/O_2$ mixtures. Their origin has been ascertained by investigating in the FT-ICR cell the reactivity of their isolated ionic precursors toward the neutrals present in the plasma. Collision-induced dissociation (CID) experiments on the $[H_n, O, Xe]^+$ (n = 1, 2) product ions are consistent with the $XeOH_n^+$ (n = 1, 2) connectivities.The thermochemistry of the XeO^+ and $XeOH^+$ ions is approximately estimated from ab initio density functional calculations and from analysis of their reaction efficiency toward some selected substrates. Accordingly, $H°_f(XeOH^+)$ = ca. 237 kcal mol^{-1} and $H°_f(XeO^+)$ = ca. 289 kcal mol^{-1}. These estimates correspond to a Xe^+-O bond dissociation energy of ca. 52 kcal mol^{-1} for $XeOH^+$ and of ca. 51 kcal mol^{-1} for XeO^+. While XeO^+ proves an exceedingly powerful oxidative oxygenating agent by formally transferring the O^+ ion to substrates, such as D_2, HCl, Cl_2, H_2O, NF_3, etc., the $XeOH^+$ appears significantly less reactive toward the same compounds. However, the presence of a hydrogen atom confers to $XeOH^+$ specific reactivity properties toward fluoromethanes, provided that these have at least one H atom. In fact, the lack of mobile hydrogens in XeO^+ makes it totally unreactive toward the same fluorinated compounds.

Acknowledgment. This work was supported by the Italian Ministero della Università e della Ricerca Scientifica e Tecnologica (MURST) and the Consiglio Nazionale delle Ricerche (CNR). The authors express their gratitude to Felice Grandinetti for his interest in this work and to Fausto Angelelli and Annito Di Marzio for their technical assistance.

References and Notes

(1) Holloway, J. H. *Noble Gas Chemistry*; Meuthen, Ed., London, 1968.
(2) Bowers, M. T.; Laudenslager, J. B. *Principles of Laser Plasmas*; Bekefi G., Ed.; Wiley: New York, 1976.
(3) (a) Bartlett, N. *Proc. Chem. Soc.* **1962**, 218. (b) Turner, J. J.; Pimentel, G. C. *Science* **1963**, *140*, 974.
(4) Turbini, L. J.; Aikman, R. E.; Lagow, R. J. *J. Am. Chem. Soc.* **1979**, *101*, 5833.
(5) Bartlett, N.; Sladky, F. *Comprehensive Inorganic Chemistry*; Pergamon: Oxford, UK, 1973; Vol. 1, pp 213−330.
(6) (a) Hovey, J. K.; McMahon, T. B. *J. Am. Chem. Soc.* **1986**, *108*, 528. (b) Hovey, J. K.; McMahon, T. B. *J. Phys. Chem.* **1987**, *91*, 4560.
(7) (a) Holtz, D.; Beauchamp, J. L. *Science* **1971**, *173*, 1237. (b) Heck, A. J.; De Koning, L. J.; Nibbering, N. M. M. *J. Phys. Chem.* **1992**, *96*, 8870.
(8) Cipollini, R.; Grandinetti, F. *J. Chem. Soc., Chem. Commun.* **1995**, 773.
(9) Jarrold, M. F.; Misev, L.; Bowers, M. T. *J. Chem. Phys.* **1984**, *81*, 4369.
(10) Filippi, A.; Troiani, A.; Speranza, M. *Chem. Phys. Lett.*, in press.
(11) Kuen, I.; Howorka, F. *J. Chem. Phys.* **1979**, *70*, 595.
(12) Berkowitz, J.; Chupka, W. A. *Chem. Phys. Lett.* **1970**, *7*, 447.
(13) (a) Giles, K.; Adams, N. G.; Smith, D. *J. Phys. B* **1989**, *22*, 873. (b) Smith, D.; Adams, N. G. *Chem. Phys. Lett.* **1989**, *161*, 30.
(14) Field, F. H.; Franklin, J. L. *J. Am. Chem. Soc.* **1961**, *83*, 4509.
(15) Theard, L. P.; Hamill, W. H. *J. Am. Chem. Soc.* **1962**, *84*, 1134.
(16) Guest, M. F.; Ding, A.; Karlan, J.; Weise, J.; Hillier, I. H. *Mol. Phys.* **1979**, *38*, 1427.
(17) (a) Cacace, F.; Speranza, M. *Science* **1994**, *265*, 208. (b) Speranza, M. *Inorg. Chem.* **1996**, *35*, 6140.
(18) (a) Horvath, M.; Bilitzky, L.; Huttner, *Topics in Inorganic Chemistry*; Clark, R. J. H., Ed.; 1985; Vol. 20. (b) Mehandjiev, D.; Naidenov, A. *Ozone Sci. Eng.* **1983**, *14*, 277.
(19) Johnstone, W. M.; Mason, N. J.; Newell, W. R.; Biggs, P.; Martson, G.; Wayne, R. P. *J. Phys. B* **1992**, *25*, 3873.
(20) Gaussian 94 (Revision C.2): Frish, M. J.; Trucks, G. W.; Schlegel, H. B.; Gill, P. M. W.; Johnson, B. G.; Robb, M. A.; Cheeseman, J. R.; Keith, T. A.; Petersson, G. A.; Montgomery, J. A.; Raghavachari, K.; Al-Laham, M. A.; Zakrzewski, V. G.; Ortiz, J. V., Foresman, J. B., Cioslowski, J.; Stefanov, B. B., Nanayakkara, A.; Challacombe, M.; Peng, C. Y.; Ayala, P. Y.; Chen, W.; Wong, M. W.; Andres, J. L.; Repogle, E. S.; Gomperts, R.; Martin. R. L.; Fox, D. J.; Binkley, J. S.; Defrees, D. J.; Baker, J.; Stewart, J. P.; Head-Gordon, M.; Gonzales, C.; Pople, J. A. Gaussian, Inc., Pittsburgh, PA, 1995.
(21) Becke, A. D. *J. Chem. Phys.* **1993**, *98*, 1372, 5648.
(22) (a) Olmstead, W. N.; Brauman, J. I. *J. Am. Chem. Soc.* **1977**, *99*, 4219. (b) Ikezoe, Y.; Matsuoka, S.; Takebe, M.; Viggiano, A. A. *Gas-Phase Ion−Molecule Reaction Rate Constants through 1986*, Maruzen Company, Ltd.: Tokyo, 1987.
(23) Bartmess, J. E.; Georgiadis, R. M. *Vacuum* **1983**, *33*, 149.
(24) De Koning, L. J.; Fokkens, R. H.; Pinkse, F. A.; Nibbering, N. M. M. *Int. J. Mass Spectrom. Ion Processes* **1987**, *77*, 95.
(25) Su, T.; Chesnavich, W. J. *J. Chem. Phys.* **1982**, *76*, 5183.
(26) Meredith, C.; Quelch, G. E.; Schaefer, H. F., III *J. Am. Chem. Soc.* **1991**, *113*, 1186.
(27) Dotan, I.; Davidson, J. A.; Fehsenfeld, F. C.; Albritton, D. L. *J. Geophys. Res.* **1978**, *83*, 5414.
(28) The trace concentration of H_2O in the FT-ICR cell is estimated by determining the rate constant for the $H_2O^+ + H_2O \rightarrow H_3O^+ + OH$ reaction in the empy FT-ICR cell and by comparing the result with the average reported rate constants (1.8×10^{-9} cm^3 molecule^{-1} s^{-1}; Kebarle, P. *Ion−Molecule Reactions*, Franklin, J. L., Ed.; Butterworth: London, 1972; Vol. 1, p 330).
(29) Lias, S. G.; Bartmess, J. E.; Liebman, J. F.; Holmes, J. L.; Levin, R. D.; Mallard, W. G. *J. Phys. Chem. Ref. Data* **1988**, *17* (Suppl. 1).
(30) We gratefully acknowledge one of the referees, who kindly provided us with some of the B3LYP/3-21G figures reported in Table 3.
(31) When calculated at the CCSD(T)/6-311++G**(d,f) level of theory (ref 33), the energy gap between $O(^1D)$ and $O(^3P)$ amounts to 51 kcal mol^{-1}, namely, 15 kcal mol^{-1} below that computed at the B3LYP/3-21G level of

theory (66 kcal mol^{-1}, Table 3). Thus, it is likely that this disturbing discrepancy arises from an overestimation of the stability of $O(^3P)$, when calculated at the B3LYP/3-21G level of theory.

(32) Li, W. K.; Ng, C. Y. *J. Phys. Chem.* **1997**, *101*, 113.

(33) Schroder, D.; Schalley, C. A.; Goldberg, N.; Hrusak, J.; Schwarz, H. *Chem. Eur. J.* **1996**, *2*, 1235.

(34) Hydrogen transfer from HCl to $^{129}XeO^+$ to give $^{129}XeOH^+$ and Cl is 9 kcal mol^{-1} exothermic. Taking into account the association energy for the $[^{129}XeOH^+ \cdot Cl]$ adduct, the first step in sequence 33 (N = H; S = Cl) is expected to be more exothermic.

(35) Yates, B. F.; Bouma, W. J.; Radom, L. *Tetrahedron* **1986**, *42*, 6225.

(36) Cacace, F.; Pepi, F.; Grandinetti, F. *J. Phys. Chem.* **1994**, *98*, 8009.

(37) Christe, K. O. *J. Am. Chem. Soc.* **1995**, *117*, 6136.

(38) Francisco, J. S.; Sander, S. P. *J. Chem. Phys.* **1995**, *102*, 9615.

(39) (a) Del Bene, J.; Vaccaro, A. *J. Am. Chem. Soc.* **1976**, *98*, 7526. (b) Del Bene, J. *J. Am. Chem. Soc.* **1978**, *100*, 1673.